

# Suppression of collagen synthesis by Dicer gene silencing in hepatic stellate cells

FUJUN YU<sup>1\*</sup>, ZHUO LIN<sup>1\*</sup>, JIANJIAN ZHENG<sup>2</sup>, SHENMENG GAO<sup>3</sup>, ZHONGQIU LU<sup>4</sup> and PEIHONG DONG<sup>1</sup>

<sup>1</sup>Department of Infectious Diseases; <sup>2</sup>Wenzhou Key Laboratory of Surgery; <sup>3</sup>Laboratory of Internal Medicine; <sup>4</sup>Emergency Department, The First Affiliated Hospital of Wenzhou Medical University, Wenzhou, Zhejiang 325000, P.R. China

Received May 13, 2013; Accepted December 6, 2013

DOI: 10.3892/mmr.2013.1866

**Abstract.** MicroRNAs (miRNAs) have emerged as important mediators of hepatic stellate cells (HSCs) and are pivotal in the pathogenesis of liver fibrosis. Dicer, the key enzyme in the RNA interference (RNAi) pathway, is involved in cutting precursor miRNAs to functionally mature forms. Emerging evidence has demonstrated that Dicer expression is dysregulated in embryo development and tumors. In the present study, we aimed to address whether Dicer expression was correlated with the activity of HSCs. We used a recombinant lentivirus to generate short hairpin RNAs (shRNAs) targeting Dicer. The mRNA and protein expression of Dicer was effectively inhibited by three pairs of Dicer shRNA vectors, of which the shRNA1 vector exhibited the strongest inhibitory effect. The shRNA1 vector demonstrated a marked inhibitory effect on the activity of HSCs, resulting in the reduction of cell proliferation and the decrease of fibrosis-related genes, including type I collagen (Col1A1),  $\alpha$ -smooth muscle actin ( $\alpha$ -SMA) and tissue inhibitor of metalloproteinases (TIMP). The mRNA expression of Col1A1,  $\alpha$ -SMA and TIMP were decreased by 60, 56 and 49%, respectively. The protein expression was reduced by 56, 52 and 42%, respectively. Additionally, the inhibition of Dicer resulted in a decrease of miR-138, -143, -140 and -122 levels, of which miR-138 exhibited the strongest decline. The firefly luciferase reporter experiments and RT-PCR indicated that phosphatase and tension homolog deleted on chromosome 10 (PTEN), Ras GTPase activating-like protein 1 (RASAL1), acyl-CoA synthetase long-chain family member 1 (ACSL1) and p27 3' untranslated region sequences were targeted by miR-138, -143, -140 and -122, respectively. Taken together, the present study contributes important new findings for the role of Dicer-mediated miRNA processing in collagen synthesis

of HSCs, which may serve as a foundation for RNAi study of liver fibrosis *in vivo*.

## Introduction

Cirrhosis is a disease with high morbidity and mortality in China, which is caused by various factors, including chronic viral hepatitis, autoimmune hepatitis, fatty liver disease or hereditary metabolic disorders (1-4). Cirrhosis is characterized by the excessive accumulation of extracellular matrix (ECM), disrupting normal liver architecture and hepatic function (5-7). Liver fibrosis is the middle stage in the progression from chronic liver diseases to cirrhosis. Hepatic stellate cells (HSCs) as a non-parenchymal liver cell population, are the most important cell type for the production of collagens (8-10). Therefore, it is a possible therapeutic strategy to treat liver fibrosis by inhibiting the activation of HSCs.

Previous studies have indicated that microRNAs (miRNAs) are important in regulating the activity of HSCs (11-14). The molecular mechanisms underlying the biogenesis of miRNAs in mammalian cells has been studied extensively (15,16). In brief, mature miRNAs are derived from RNA molecules that are selectively cleaved by the ribonuclease Droscha, exported into the cytoplasm and cleaved again by Dicer. Consequently, Dicer is essential for the processing of miRNAs. Dysregulation of Dicer globally impairs miRNA processing and activity. Currently, Dicer is extensively studied in development and cancer. Loss of Dicer in mice disrupts embryonic stem cell differentiation and is lethal during early development (17). Additionally, Dicer is upregulated in prostate adenocarcinoma, ovarian serous carcinomas, pleomorphic adenomas of the salivary gland and acute myeloid leukemia (18-21). By contrast, it has been demonstrated that Dicer is downregulated in hepatocellular carcinoma (HCC). Reduced Dicer expression is associated with the poor prognosis of patients with HCC (22). In summary, these findings imply that the knock-down of Dicer may be involved in tumorigenesis. However, whether Dicer expression is associated with liver fibrosis is yet to be determined.

Our previous experiment demonstrates that the expression of Dicer is upregulated in liver fibrosis. The purpose of the present study was to utilize an RNA interfering (RNAi) technique to explore the effect of Dicer gene silencing on the activity of HSCs. Our results demonstrated that Dicer downregulation

---

*Correspondence to:* Dr Peihong Dong, Department of Infectious Diseases, The First Affiliated Hospital of Wenzhou Medical University, no. 2 Fuxue Lane, Wenzhou, Zhejiang 325000, P.R. China  
E-mail: ktsqdp@163.com

\*Contributed equally

**Key words:** Dicer, microRNA, liver fibrosis, hepatic stellate cells, short hairpin RNA

inhibits the activity of HSCs through the reduction of miRNAs associated with liver fibrosis. Our findings reveal that Dicer is pivotal in the progression of liver fibrosis.

## Materials and methods

**Design of shRNA.** Target gene Dicer (accession no. XM\_001068155.3) was searched from GenBank. According to Ambion's principles of short hairpin RNA (siRNA) design, three sequences of 19 nucleotides containing 30-50% GC were selected and used as the target sites. Their sequences are listed in Table I. Another unrelated sequence was used as a negative control. No homology sequence was identified on BLAST analysis. The shRNA was as follows: *Bam*HI + sense + loop + antisense + stop signal + *Bbs*I. Single-stranded DNA oligonucleotide was synthesized and annealed to form double strands by Shanghai GenePharma Co., Ltd. (Shanghai, China).

**Lentiviral preparation and transfection of HSC-T6 cells.** Three lentiviral pGLV1-1 shRNA vectors and a negative vector (shRNA non-related vector) were constructed by Shanghai GenePharma Co., Ltd. With 293T cells, the pGLV1-1 and negative shRNA vectors were packaged into concentrated lentiviruses by a three plasmid transfection procedure. Viral titers were estimated with a Lenti-X qRT-PCR kit (Chemicon, Billerica, MA, USA) and typically averaged  $1 \times 10^9$  viral genomes/ml. Rat HSC-T6 cells (Chinese Academy of Medical Science, Beijing, China) were cultured in Dulbecco's modified Eagle's medium supplemented with 10% fetal bovine serum (Invitrogen Life Technologies, Carlsbad, CA, USA). Then cells were transfected with pGLV1-1 shRNA vectors according to the manufacturer's instructions. In brief,  $\sim 1 \times 10^5$  cells were plated on a 6-well dish 24 h prior to transfection. HSCs were transfected at a multiplicity of infection (MOI) of 5. Transfection efficiency was determined to be >90% by direct visualization of green fluorescent protein (GFP) expression following transfection for 48 h. The transfected cells were selected by adding 2  $\mu$ g/ml of puromycin to the media for 1-2 weeks.

**Quantitative real-time PCR.** Total RNA was isolated from HSC-T6 cells using the mirVana miRNA extraction kit (Ambion, Austin, TX, USA) according to the manufacturer's instructions. With the ReverTra Ace qPCR RT kit (Toyobo Co., Ltd., Osaka, Japan), 50 ng of total RNA was reverse transcribed to cDNA. The mRNA expression was determined by real-time PCR using cDNA, SYBR-Green real-time PCR Master mix (Toyobo Co., Ltd.) and a set of gene-specific oligonucleotide primers (Table II). To detect miRNA expression, the reverse transcription and real-time PCR reaction was performed using the TaqMan MicroRNA Assay (Applied Biosystem, Foster, CA, USA) according to the manufacturer's instructions. The glyceraldehyde 3-phosphate dehydrogenase (GAPDH) and U6 shRNA levels were measured and used to normalize the relative abundance of mRNAs and miRNAs, respectively. The expression levels of mRNAs and miRNAs were calculated by the  $2^{-\Delta\Delta C_t}$  method.

**Protein extraction and western blot analysis.** Proteins were separated on sodium dodecyl sulfate-polyacrylamide gel electrophoresis (SDS-PAGE) and then transferred onto

Table I. Predesigned siRNAs for rat Dicer.

Name	Sequence (DNA)
siRNA1	GCTACACAGGAAGTTCTTA
siRNA2	GGGAAAGTCTGCAGAACAA
siRNA3	CCTCATAACCAAGCACCTT

siRNAs, short hairpin RNAs.

Table II. List of primer sequences.

Gene		Sequence (5'-3')
<i>Dicer</i>	Forward	CGATAACTTTATTGGAGATTTAC
	Reverse	ATTGGGTGTCCCAGAGATT
<i>Type 1 collagen</i>	Forward	CCTGGCAAAGACGGACTCAAC
	Reverse	GCTGAAGTCATAACCGCCACTG
<i><math>\alpha</math>-SMA</i>	Forward	TCCCTGGAGAAGAGCTACGAACT
	Reverse	AAGCGTTTCGTTTCCAATGGT
<i>TIMP-1</i>	Forward	CCTCTGGCATCTCTTGTGCTAT
	Reverse	CATTCCCACAGCGTCGAATCCTT
<i>PTEN</i>	Forward	GTGGTCTGCCAGCTAAAGGT
	Reverse	TGTCACCACACACAGGCAAT
<i>RASAL1</i>	Forward	CTCCTGGGCATGGTGGAAT
	Reverse	CACGGACTCCAGAAGCAGTT
<i>ACSL1</i>	Forward	TGTGGGGTGGAAATCATCGG
	Reverse	CATTGCTCCTTTGGGGTTGC
<i>p27</i>	Forward	AGATACGAGTGGCAGGAGGT
	Reverse	ATGCCGGTCTCAGAGTTTG
<i>GAPDH</i>	Forward	TGCACCACCAACTGCTTAG
	Reverse	GGATGCAGGGATGATGTTT

$\alpha$ -SMA,  $\alpha$ -smooth muscle actin; TIMP-1, tissue inhibitor of metalloproteinases-1; RASAL1, Ras GTPase activating-like protein 1; GAPDH, glyceraldehyde 3-phosphate dehydrogenase; PTEN, phosphatase and tension homolog deleted on chromosome 10; ACSL1, acyl-CoA synthetase long-chain family member 1.

nitrocellulose membranes. Following blocking, the membranes were incubated with primary antibodies, followed by the appropriate secondary antibodies (Maixin, Fuzhou, Fujian, China). The primary antibodies included: rabbit polyclonal anti-type I collagen, anti-GAPDH, mouse monoclonal anti- $\alpha$ -smooth muscle actin ( $\alpha$ -SMA; Abcam, Cambridge, MA, USA) and rabbit polyclonal anti-Dicer (Santa Cruz Biotechnology, Inc., Santa Cruz, CA, USA). Immunoreactive bands were visualized by the enhanced chemiluminescence substrate using the Fujifilm Image Reader LAS-3000 (Fuji Medical Systems, Stamford, CT, USA).

**Cell proliferation assays.** The cell proliferation was measured by the WST-1 assay (Beyotime Institute of Biotechnology, Shanghai, China) based on changes in absorbance at 450 nm. Cells were seeded in a 24-well plate at a density of  $1 \times 10^4$  cells/well. Then cells were transfected with Dicer

shRNAs and incubated for 48 h prior to the assessment of cell proliferation. The optical density (OD) at 450 nm was determined using a microplate reader and the proliferation ability was calculated as the experimental OD value/control OD value. The experiments were implemented in triplicate.

**Luciferase activity assay.** 3'UTRs containing putative miRNA target regions of phosphatase and tension homolog deleted on chromosome 10 (PTEN), Ras GTPase activating-like protein 1 (RASAL1), acyl-CoA synthetase long-chain family member 1 (ACSL1) and p27 genes were obtained by PCR using rat HSCs cDNA as a template. Primers were as follows: PTEN-miR-29c, forward 5'-GGACTAGTTGGTGCTAGAAAAGGCAGCTA-3', and reverse 5'-AGCTTTGTTTAAACAACGGCTGACAGCTATTGAA-3'; RASAL1-miR-143, forward 5'-GGACTAGTATTCCAGAAACGGGGCTAGG-3' and reverse 5'-AGCTTTGTTTAAACGTATATTGTCTAGATTAA-3'; ACSL1-miR-214, forward, 5'-GGACTAGTTCTTACCCCTTCCCCTTGT-3' and reverse 5'-AGCTTTGTTTAAACGGGAGGAATCACAGTTGAGC-3'; and p27-miR-199a-5p, forward 5'-GGACTAGTGATTCGTATTGTAGCAAGAAATGG-3' and reverse 5'-AGCTTTGTTTAAACAGTAGGGTGAGACACTTTGAATTT-3'. Each of the forward and reverse primers carried the *SpeI* and *PmeI* sites at their 5'-ends. The obtained DNA fragments were inserted into the pMIR-reporter vector. The pMIR-reporter vector without the insert was used as a negative control. pMIR-reporter  $\beta$ -gal control plasmid was used for transfection normalization. HSCs were cultured in 24-well plates and transfected with 800 ng of reporter vector along with 100 ng of pMIR- $\beta$ -gal and 20 pmol of miRNA precursors. Lipofectamine™ 2000 (Invitrogen Life Technologies) was used as the transfection reagent. Following transfection 48 h later, luciferase and  $\beta$ -gal activity were measured using the Dual-Light System.

**Statistical analysis.** Data from three independent experiments are expressed as the mean  $\pm$  SD. The difference between groups was calculated using the Student's t-test when two groups were compared. All tests performed were two sided.  $P < 0.05$  was considered to indicate a statistically significant difference.

## Results

**Inhibition of Dicer expression by lentivirus.** We constructed a recombinant lentivirus to generate shRNAs targeting Dicer. The Dicer expression was determined by real-time RT-PCR and western blotting following transfection of HSCs with pGLV1-1 shRNA vectors. Following 48 h, green fluorescence was observed in the transfected cells under the fluorescence microscope, the transfection efficiency being  $\sim 91\%$ . It was identified that the shRNA groups had significantly lower mRNA expression of Dicer than the control group (Fig. 1A), of which the shRNA1 group exhibited the strongest inhibitory effect. In addition, western blot analysis demonstrated a marked decrease in the protein expression of Dicer, of which the shRNA1 group exhibited the strongest inhibitory effect (Fig. 1B and C). However, there was no change in the negative group. It was concluded that the mRNA and protein expression of Dicer was effectively inhibited by shRNA vectors. Based

on its inhibitory effect, we selected the shRNA1 group as the object of the next experiments.

**Effect of Dicer shRNA on type I collagen and  $\alpha$ -SMA expression.** In the progression of liver fibrosis, HSCs can express an abundance of type I collagen and  $\alpha$ -SMA. Consequently, we examined the effect of Dicer shRNA on type I collagen and  $\alpha$ -SMA expression. Compared with the control group, the shRNA1 group presented the significant inhibition of Col1A1 and  $\alpha$ -SMA mRNA expression, which was decreased by  $\sim 60$  and  $56\%$ , respectively (Fig. 2A). By contrast, the negative group had a negligible effect on them. Additionally, we determined the effect of Dicer gene silencing on type I collagen and  $\alpha$ -SMA protein expression. Consistent with the real-time RT-PCR results, the protein expression of type I collagen and  $\alpha$ -SMA were reduced by  $\sim 56$  and  $52\%$ , respectively (Fig. 2B and C), while there was no decline in the negative group.

**Effect of Dicer gene silencing on the expression of tissue inhibitor of metalloproteinases-1 (TIMP-1).** A high level of TIMP-1 in liver fibrosis accounts for the slow degradation of ECM. Accordingly, we monitored TIMP-1 mRNA and protein expression in HSC-T6 cells following transfection with Dicer shRNA. Compared with the control group, loss of Dicer markedly inhibited TIMP-1 mRNA and protein expression, which was suppressed by  $\sim 49$  and  $42\%$ , respectively (Fig. 3). Nevertheless, the negative group did not demonstrate a statistical change in TIMP-1 expression. These results suggested that the knockdown of Dicer may treat liver fibrosis by degrading the deposition of ECM.

**Cell proliferation evaluated by WST-1 assay.** Activated HSCs are known to acquire proliferation ability. We considered the possibility that the inhibition of Dicer was able to regulate the proliferation of HSCs. As shown by the WST-1 assay, shRNA1 inhibition of HSC proliferation was decreased by  $28\%$  relative to the control (Fig. 4). Meanwhile, there was no difference between the negative and control group. Therefore, we concluded that the knockdown of Dicer inhibited the proliferation of HSCs.

**Effect of Dicer shRNA on miRNAs.** Dicer is critical for the biogenesis of miRNAs. To determine whether the inhibition of Dicer in HSC-T6 cells could affect miRNAs biogenesis, we performed real-time RT-PCR on RNA isolated from cultures transfected with the shRNA1 vector. We decided to test a set of specific miRNAs that were markedly different between the activated and quiescent HSCs, as previously described from microarray profiles (23). The inhibition of Dicer resulted in a decrease in the expression of miR-214, -143, -29c and -199a-5p, of which miR-214 exhibited the strongest decline (Fig. 5). In comparison, we did not detect a statistically significant change in miR-19b or miR-99a, indicating that not all miRNAs were affected by the reduction of Dicer. These data revealed that the antifibrotic effect of Dicer was mainly implemented by the majority of fibrosis-related miRNAs.

**Interaction of miR-214, -143, -29c and -199a-5p with 3'UTRs of ACSL1, RASAL1, PTEN and p27 mRNAs.** The question of how miRNAs functioned in blocking HSCs activation was also examined. We firstly investigated what the targets of miR-214,

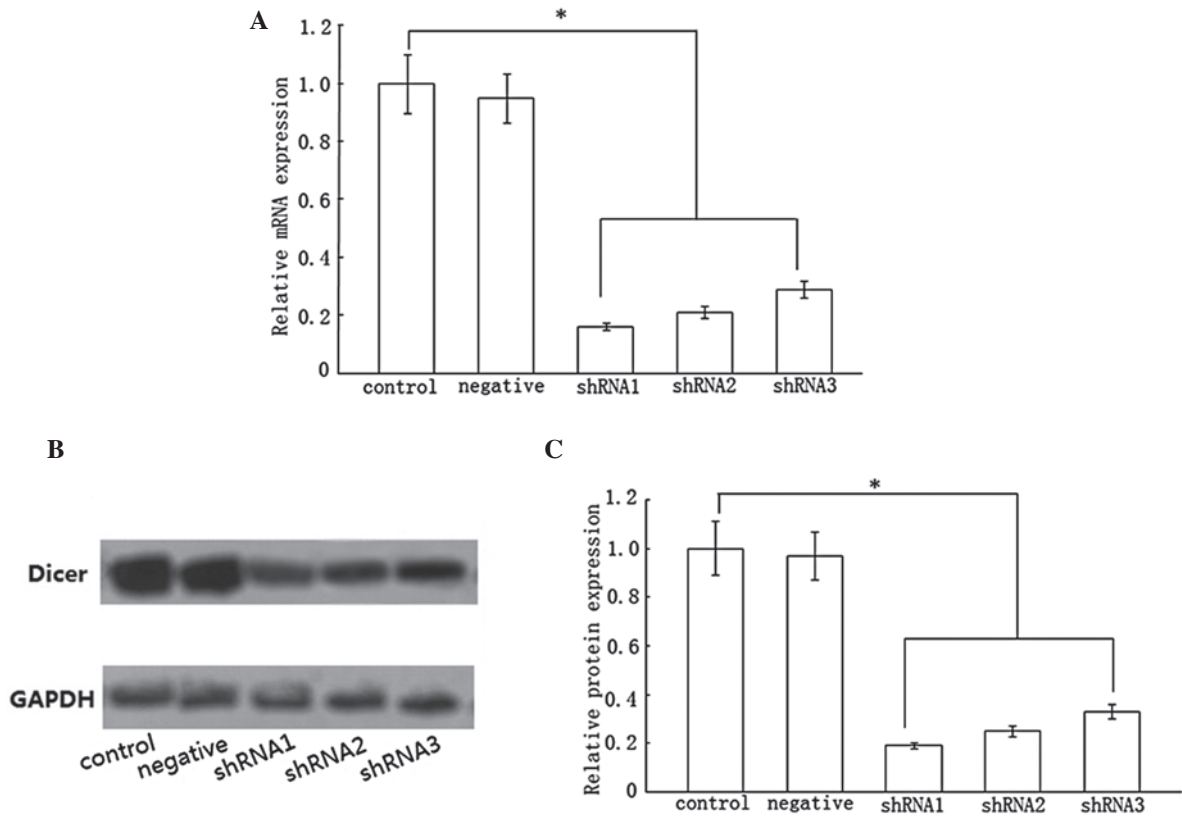


Figure 1. Effect of three pairs of shRNA vectors on Dicer. Three pairs of shRNA vectors were transfected into HSCs for 48 h. Compared with the control group, Dicer mRNA expression was decreased in the shRNA1, shRNA2 and shRNA3 groups by ~84, 79 and 71%, respectively. Dicer protein expression was reduced in shRNA1, shRNA2 and shRNA3 groups by ~81, 75 and 67%, respectively. (A and C) Statistical analysis. (B) Results of western blotting. Data represent the results from three independent experiments. \* $P < 0.05$  compared with the control. shRNA, short hairpin RNA; HSCs, hepatic stellate cells; GAPDH, glyceraldehyde 3-phosphate dehydrogenase.

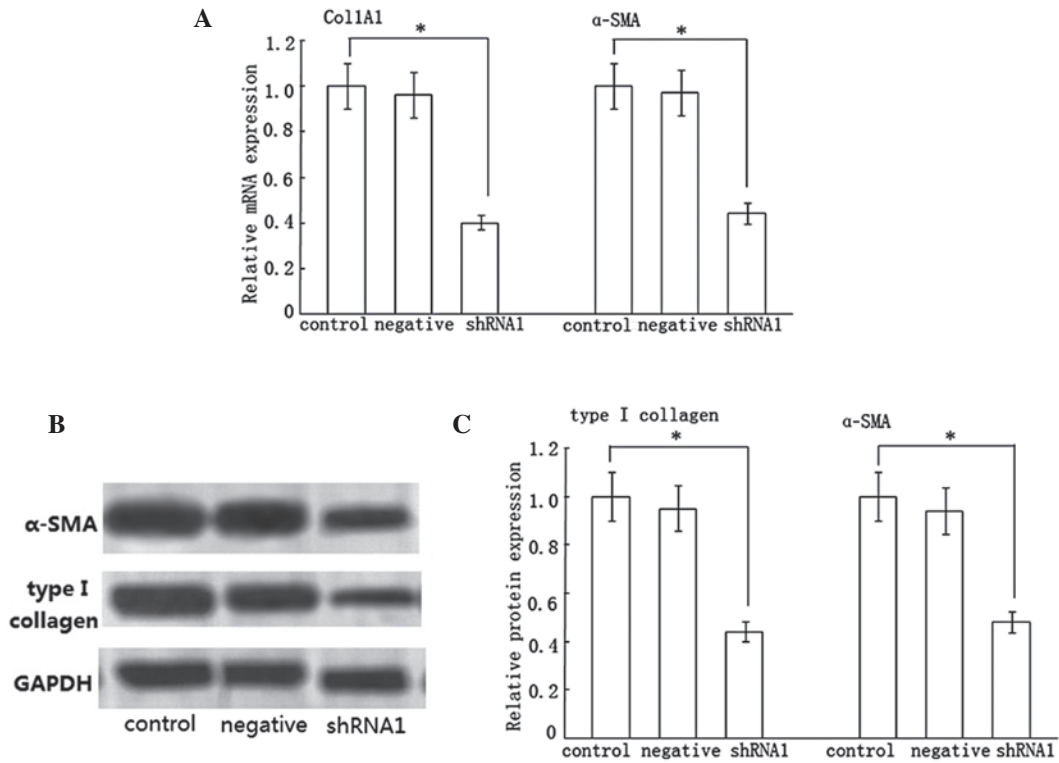


Figure 2. Effect of the shRNA1 vector on Col1A1 and  $\alpha$ -SMA expression. (A and C) Statistical analysis. (B) Results of western blotting. Data represent the results from three independent experiments. \* $P < 0.05$  compared with the control. shRNA, short hairpin RNA; Col1A1, type I collagen;  $\alpha$ -SMA,  $\alpha$ -smooth muscle actin; GAPDH, glyceraldehyde 3-phosphate dehydrogenase.

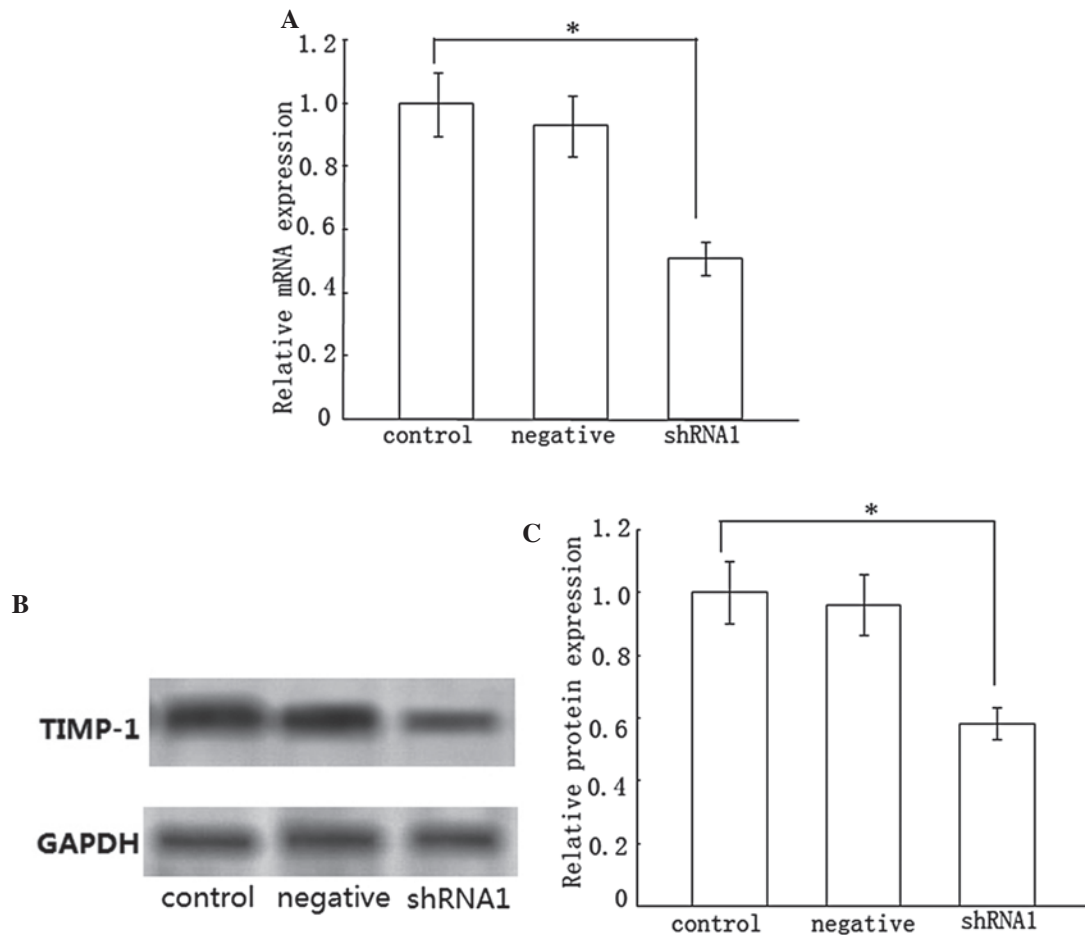


Figure 3. Effect of the shRNA1 vector on TIMP-1 expression. (A and C) Statistical analysis. (B) Results of western blotting. Data represent the results from three independent experiments. \* $P < 0.05$  compared with the control. shRNA, short hairpin RNA; TIMP-1, tissue inhibitor of metalloproteinases-1; GAPDH, glyceraldehyde 3-phosphate dehydrogenase.

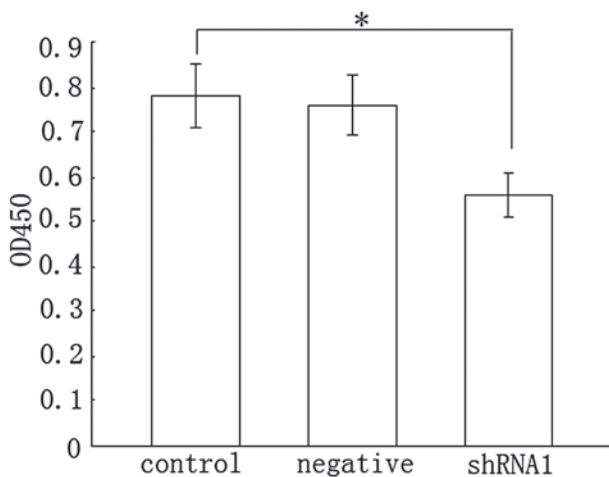


Figure 4. Cell proliferation was evaluated by the WST-1 assay. Data represent the results from three independent experiments. \* $P < 0.05$  compared with the control. shRNA, short hairpin RNA.

-143, -29c and -199a-5p were. The prediction of miRNA target regions by bioinformatics indicated that ACSL1, RASAL1, PTEN and p27 3'UTR had one target region for miR-214, -143, -29c and -199a-5p, respectively. To explore the direct targeting of ACSL1 by miR-214, the sequence of the target region was

cloned and inserted into the downstream region of the firefly luciferase reporter gene. Then the vector was cotransfected into rat HSCs with miRNA precursors or negative control precursors. Compared with the negative control precursors, the miR-214 precursors decreased luciferase activity in pMIR containing the miR-214 target sequence (pMIR-3'UTR), whereas there were no changes in pMIR empty vector (pMIR) and pMIR with miR-214 mutant target sequence (pMIR-mut 3'UTR; Fig. 6A). In a similar way, the miR-143, -29c and -199a-5p precursors also lowered luciferase activities of the vectors carrying the respective miRNA target sequence (Fig. 6B-D). Based on these observations, we inferred that PTEN, RASAL1, ACSL1 and p27 3'UTR sequences could be targeted by miR-29c, -143, -214 and -199a-5p, respectively. To confirm the results, we measured endogenous PTEN, RASAL1, ACSL1 and p27 levels in HSC-T6 cells expressing miR-29c, -143, -214 and -199a-5p inhibitors, respectively. RT-PCR analyses of whole cell extracts suggested that the steady-state levels of PTEN, RASAL1, ACSL1 and p27 were elevated by ~210, 95, 150 and 70%, respectively (Fig. 7).

## Discussion

Dicer, the key enzyme in the RNAi pathway, is required for the processing of miRNA precursors into mature miRNA

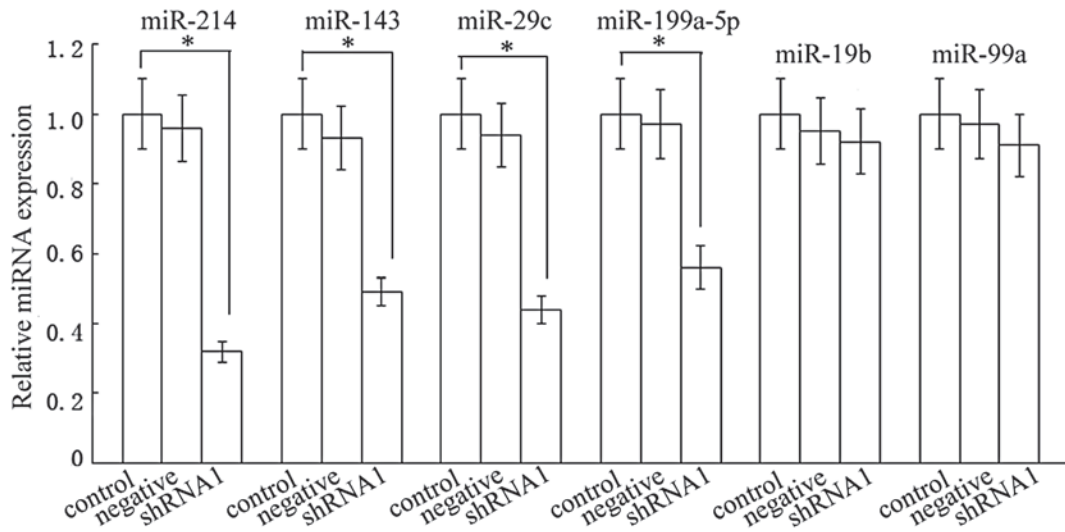


Figure 5. Effect of the shRNA1 vector on miRNA expression. Real-time RT-PCR was performed on RNA isolated from shRNA transfected HSCs. Compared with the control group, the levels of miR-214, -143, -29c and -199a-5p in the shRNA1 group were reduced by ~68, 51, 56 and 44%, respectively. (n=3, \*P>0.05). The levels of miR-19b or miR-99a were not significantly affected (n=3, P>0.05). shRNA, short hairpin RNA; RT-PCR, reverse transcription polymerase chain reaction; HSCs, hepatic stellate cells.

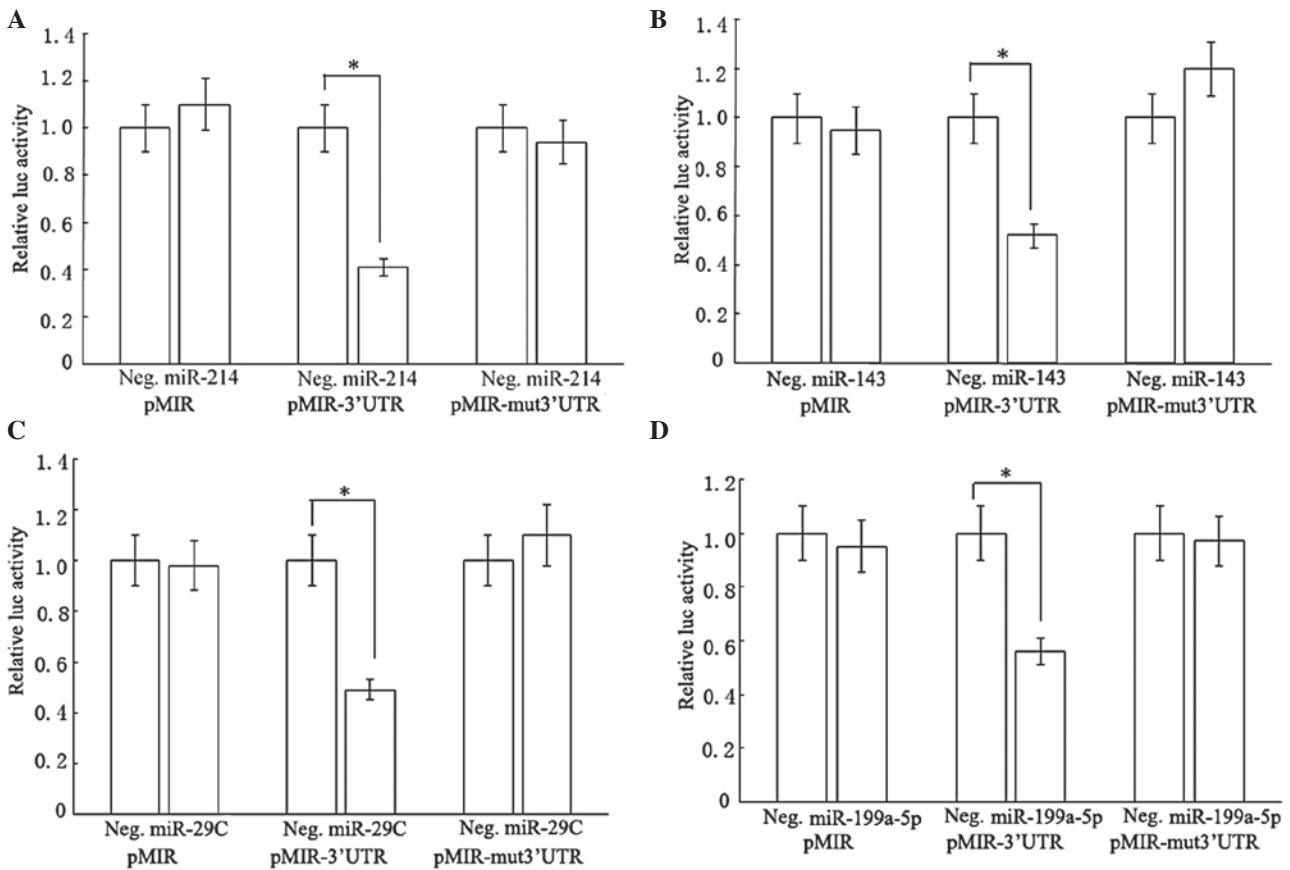


Figure 6. Luciferase activities controlled by target regions are inhibited by miRNA precursors. Neg., cotransfection of reporter vectors along with negative control precursors, which have a scrambled sequence. miRNA, cotransfection of reporter vectors along with miRNA precursors. Data represent the results from three independent experiments. \*P<0.05. miRNA, microRNA.

molecules. In the present study, we investigated the effect of reducing the miRNA biogenesis enzyme Dicer on the activity of HSCs. In the present study, we investigated

several lead proteins that may represent the activation of HSCs. In response to inflammatory stimuli, HSCs activate and become myofibroblastic cells that express  $\alpha$ -SMA as a

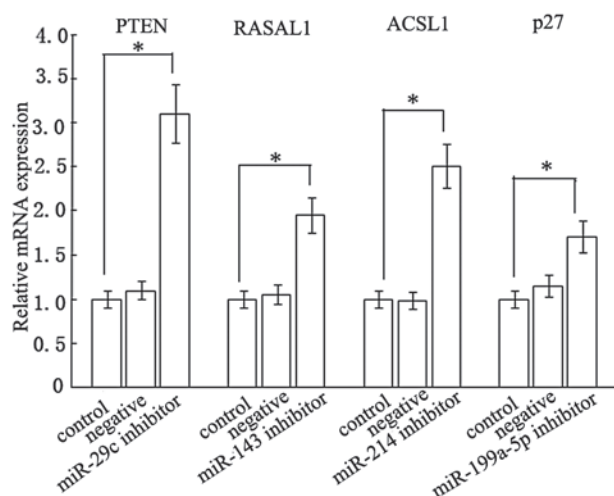


Figure 7. The levels of phosphatase and PTEN, RASAL1, ACSL1 and p27 are increased by respective miRNA inhibitors. Data represent the results from three independent experiments. \*P<0.05 compared with the control. PTEN, tension homolog deleted on chromosome 10; RASAL1, ras GTPase activating-like protein 1; ACSL1, acyl-CoA synthetase long-chain family member 1; miRNA, microRNA.

representative marker (24). In the progression of liver fibrosis, the leading ECM proteins become type I collagen instead of type III collagen. Therefore, type I collagen is a good indicator representing the deposition of ECM. Our results indicate that the mRNA and protein expression of type I collagen and  $\alpha$ -SMA are markedly decreased by Dicer gene silencing. These findings raise the possibility that a reduction in Dicer contributes to the downregulation of fibrosis-related genes. Taken together, these results suggest that Dicer inhibition is able to suppress HSC activation as well as ECM expression.

A second major biological consequence of Dicer knockdown is the inhibition of TIMP1. Matrix metalloproteinases (MMPs) are a family of enzymes responsible for the proteolytic processing of ECM structural proteins, an essential step in the treatment of liver fibrosis (25). TIMP-1 can inhibit the activity of MMPs, thus accelerating the progression of liver fibrosis. Our results suggested that the mRNA and protein expression of TIMP1 was significantly lowered by Dicer loss. Therefore, we conclude that impaired miRNA processing enhances the metastatic potential. These findings may have significant clinical value.

Although the disruption of Dicer has been associated with the reduced activity of HSCs, the mechanisms of this event remain elusive. In the present study, we began to investigate several miRNAs that were associated with liver fibrosis. Post-transcriptional regulation of gene expression by miRNAs is pivotal in a wide variety of cellular processes. In the present study, we identified an association between the downregulation of Dicer and the expression of miRNAs. The present study demonstrates that the downregulation of a key component in the miRNA processing machinery decreases the expression of certain miRNAs. These specific miRNAs were selected based on previously published miRNA microarrays, which identified these miRNAs as of potential interest in liver fibrosis (23). Notably, not all tested miRNAs were reduced, presenting either high basal expression levels or

long half-lives. Taken together, these data reveal that global miRNA loss is responsible for the antifibrotic effect of Dicer knockdown.

The functions of miRNA have been gradually uncovered. The prediction of miRNA target regions currently depends mainly on bioinformatics programs. Since each miRNA is able to control numerous target genes, its function can be explained as the sum of the functions of the genes it regulates. The activation of PI3K signaling is a pivotal event during HSC activation. PTEN is a negative regulator of PI3K signaling and thus the elevated PTEN can block PI3K activity and prevent the activation of HSCs into fibrogenic cells (26,27). RASAL1, a member of the RAS-GAP family, is critical in the constitutive activity of Ras signaling. It has been previously demonstrated that the decreased expression of RASAL1 contributes to liver fibrosis progression (28,29). ACSL1 is crucial in lipid metabolism and fatty acid metabolism in the liver. Li *et al* (29) indicated that the reduced amounts of ACSL1 in the liver blocked the partitioning of fatty acids to triglyceride storage and by doing so contributed to the progression of hepatic fibrosis. p27, a key inhibitor of the cell cycle, can lower the proliferation of HSCs and cell cycle progression by increasing the number of S phase cells (30). An assay of luciferase activity in a luminometer using the Dual-Light System indicates that ACSL1, RASAL1, PTEN and p27 are targets of miR-214, -143, -29c and -199a-5p, respectively. We observed that, when HSCs were transfected with the respective miRNA inhibitor, the levels of ACSL1, RASAL1, PTEN and p27 were increased accordingly. In agreement with these studies, we revealed a significant reduction in these miRNAs upon Dicer shRNA transfection. It is hypothesized that the upregulation of target mRNA levels induced by corresponding miRNA inhibitors presumably blocks the activation of HSCs, which explains the antifibrotic effect of Dicer shRNA.

Although  $\alpha$ -SMA and TIMP-1 are not predicted targets of the above miRNAs, their mRNA and protein levels were suppressed. Thus, this effect was thought to be a secondary action of miRNA inhibition. That is, it is suggested that miRNAs can not only impede the expression of target regions, but also suppress the activation of HSCs by regulating other unidentified mechanisms, resulting in the inhibition of  $\alpha$ -SMA and TIMP-1.

In summary, the present study suggests for the first time, to the best of our knowledge, that Dicer gene silencing can inhibit collagen synthesis in HSCs. Importantly, our study contributes important new findings for the role of Dicer-mediated miRNA processing in the collagen synthesis of HSCs. Targeted delivery of Dicer to activated HSCs in the liver may become a new therapeutic strategy for liver fibrosis in the future.

#### Acknowledgements

This study was supported by the National Natural Science Foundation of China (nos. 81000176/H0317, 81100292/H0317 and 81200350), the Zhejiang Provincial Natural Science Foundation of China (nos. Y2090326, Y2110634 and LY12H08003), the Wang Bao-En Liver Fibrosis Foundation (nos. 20100002 and 20120127), the Wenzhou Municipal

Science and Technology Bureau (no. Y20110033), the Zhejiang Extremely Key Subject of Surgery and the Key Disciplines in Colleges and Universities of Zhejiang Province.

## References

- Hsu YC, Lin JT, Chen TT, Wu MS and Wu CY: Long-term risk of recurrent peptic ulcer bleeding in patients with liver cirrhosis: a 10-year nationwide cohort study. *Hepatology* 56: 698-705, 2012.
- Li L, Yu C and Li Y: Endoscopic band ligation versus pharmacological therapy for variceal bleeding in cirrhosis: a meta-analysis. *Can J Gastroenterol* 25: 147-155, 2011.
- Qin T, Xia J, Ren H, Zhou H, Tang B and Shao Z: Liver cirrhosis as a predisposing condition for Legionnaires' disease: a report of four laboratory-confirmed cases from China. *J Med Microbiol* 61: 1023-1028, 2012.
- Wang SB, Wang JH, Chen J, Giri RK and Chen MH: Natural history of liver cirrhosis in south China based on a large cohort study in one center: a follow-up study for up to 5 years in 920 patients. *Chin Med J (Engl)* 125: 2157-2162, 2012.
- Giannone FA, Baldassarre M, Domenicali M, *et al*: Reversal of liver fibrosis by the antagonism of endocannabinoid CB1 receptor in a rat model of CCl(4)-induced advanced cirrhosis. *Lab Invest* 92: 384-395, 2012.
- Madro A, Czechowska G, Slomka M, Celinski K, Szymonik-Lesiuk S and Kurzepa J: The decrease of serum MMP-2 activity corresponds to alcoholic cirrhosis stage. *Alcohol* 46: 155-157, 2012.
- Wirkowska A and Paczek L: Liver fibrosis and cirrhosis--selected cytokines, growth factors and proteins. Part II. *Przegl Lek* 68: 228-230, 2011 (In Polish).
- Oliveira-Junior MC, Monteiro AS, Leal-Junior EC, *et al*: Low-level laser therapy ameliorates CCl(4)-induced liver cirrhosis in rats. *Photochem Photobiol* 89: 173-178, 2013.
- Lee JK, Kim JH and Shin HK: Therapeutic effects of the oriental herbal medicine Sho-saiko-to on liver cirrhosis and carcinoma. *Hepatol Res* 41: 825-837, 2011.
- Cao S, Yaqoob U, Das A, *et al*: Neuropilin-1 promotes cirrhosis of the rodent and human liver by enhancing PDGF/TGF-beta signaling in hepatic stellate cells. *J Clin Invest* 120: 2379-2394, 2010.
- Iizuka M, Ogawa T, Enomoto M, *et al*: Induction of microRNA-214-5p in human and rodent liver fibrosis. *Fibrogenesis Tissue Repair* 5: 12, 2012.
- He Y, Huang C, Sun X, Long XR, Lv XW and Li J: MicroRNA-146a modulates TGF-beta1-induced hepatic stellate cell proliferation by targeting SMAD4. *Cell Signal* 24: 1923-1930, 2012.
- Noetel A, Kwiecinski M, Elfimova N, Huang J and Odenthal M: microRNA are central players in anti- and profibrotic gene regulation during liver fibrosis. *Front Physiol* 3: 49, 2012.
- Ogawa T, Enomoto M, Fujii H, *et al*: MicroRNA-221/222 upregulation indicates the activation of stellate cells and the progression of liver fibrosis. *Gut* 61: 1600-1609, 2012.
- Dueck A, Ziegler C, Eichner A, Berezikov E and Meister G: microRNAs associated with the different human Argonaute proteins. *Nucleic Acids Res* 40: 9850-9862, 2012.
- Gurtan AM, Lu V, Bhutkar A and Sharp PA: In vivo structure-function analysis of human Dicer reveals directional processing of precursor miRNAs. *RNA* 18: 1116-1122, 2012.
- Andersson T, Rahman S, Sansom SN, *et al*: Reversible block of mouse neural stem cell differentiation in the absence of dicer and microRNAs. *PLoS One* 5: e13453, 2010.
- Chiosea S, Jelezcova E, Chandran U, *et al*: Up-regulation of dicer, a component of the MicroRNA machinery, in prostate adenocarcinoma. *Am J Pathol* 169: 1812-1820, 2006.
- Vaksman O, Hetland TE, Tropé CG, Reich R and Davidson B: Argonaute, Dicer, and Drosha are up-regulated along tumor progression in serous ovarian carcinoma. *Hum Pathol* 43: 2062-2069, 2012.
- Zhang X, Cairns M, Rose B, *et al*: Alterations in miRNA processing and expression in pleomorphic adenomas of the salivary gland. *Int J Cancer* 124: 2855-2863, 2009.
- Martin MG, Payton JE and Link DC: Dicer and outcomes in patients with acute myeloid leukemia (AML). *Leuk Res* 33: e127, 2009.
- Wu JF, Shen W, Liu NZ, *et al*: Down-regulation of Dicer in hepatocellular carcinoma. *Med Oncol* 28: 804-809, 2011.
- Lakner AM, Steuerwald NM, Walling TL, *et al*: Inhibitory effects of microRNA 19b in hepatic stellate cell-mediated fibrogenesis. *Hepatology* 56: 300-310, 2012.
- Uyama N, Iimuro Y, Kawada N, *et al*: Fascin, a novel marker of human hepatic stellate cells, may regulate their proliferation, migration, and collagen gene expression through the FAK-PI3K-Akt pathway. *Lab Invest* 92: 57-71, 2012.
- Ramachandran P and Iredale JP: Liver fibrosis: a bidirectional model of fibrogenesis and resolution. *QJM* 105: 813-817, 2012.
- Takashima M, Parsons CJ, Ikejima K, Watanabe S, White ES and Rippe RA: The tumor suppressor protein PTEN inhibits rat hepatic stellate cell activation. *J Gastroenterol* 44: 847-855, 2009.
- Bian EB, Huang C, Ma TT, *et al*: DNMT1-mediated PTEN hypermethylation confers hepatic stellate cell activation and liver fibrogenesis in rats. *Toxicol Appl Pharmacol* 264: 13-22, 2012.
- Tao H, Huang C, Yang JJ, *et al*: MeCP2 controls the expression of RASAL1 in the hepatic fibrosis in rats. *Toxicology* 290: 327-333, 2011.
- Li WQ, Chen C, Xu MD, *et al*: The rno-miR-34 family is upregulated and targets ACSL1 in dimethylnitrosamine-induced hepatic fibrosis in rats. *FEBS J* 278: 1522-1532, 2011.
- Wang B, Li W, Guo K, Xiao Y, Wang Y and Fan J: miR-181b promotes hepatic stellate cells proliferation by targeting p27 and is elevated in the serum of cirrhosis patients. *Biochem Biophys Res Commun* 421: 4-8, 2012.